Mesoporous Materials

DOI: 10.1002/ange.200504114

Synthesis and Characterization of Mesoporous Silica AMS-10 with Bicontinuous Cubic *Pn*$\bar{3}$*m* Symmetry**

*Chuanbo Gao, Yasuhiro Sakamoto,**
*Kazutami Sakamoto, Osamu Terasaki, and Shunai Che**

It is well known that various mesoporous materials can be synthesized based on the self-assembly of surfactant and inorganic precursors. Mesoporous materials have attracted a great deal of attention because of their controllable structures and compositions, which make them suitable for wide applications in catalysis, environmental clean-up, and in the design of advanced materials. Since the first reports of mesoporous materials (FSM-16[1] and M41S family[2]) by Yanagisawa et al. and Mobil Research, respectively, a variety of other phases have been reported. Until now, many well-ordered mesoporous materials have been successfully synthesized and it has been claimed that these have different mesostructures such as orthorhombic (*Pmmm*[3] etc.), tetragonal ($P4_2/mnm$,[4] $P4/mmm$[3]), three-dimensional (3D) hexagonal ($P6_3/mmc$[5]), micellar cubic ($Pm\bar{3}n$,[6,7] $Fd\bar{3}m$,[8,9] $Im\bar{3}m$,[7,10] $Fm\bar{3}m$,[11] $Pm\bar{3}m$,[10] etc.), bicontinuous cubic ($Ia\bar{3}d$,[2,12] $Im\bar{3}m$[13] and $Pn\bar{3}m$[14]), rectangular ($c2mm$[15]), two-dimensional (2D) hexagonal ($p6mm$[2,16]), and lamellar phase.[2] Most structures have been proposed on the basis of a combination of powder X-ray diffraction (XRD) studies and an accumulated knowledge of liquid-crystalline phases, whilst only a few have been precisely determined by electron crystallography. Elaborate synthesis under well-controlled conditions and careful structural studies are required to form mesoporous crystals with the $Pn\bar{3}m$ space group.

Recently, we reported the preparation of ordered mesoporous structures using anionic surfactants and co-structure-directing agents (CSDAs).[17] The introduction of CSDAs into the reaction system makes it feasible to produce electrostatic interactions between anionic surfactants and inorganic species and to control the packing parameter. These are key factors in the formation of highly ordered mesophases and to select a certain structure. Various mesophases, including lamellar, 2D hexagonal *p6mm*, tetragonal $P4_2/mnm$, 3D hexagonal $P6_3/mmc$, cubic $Pm\bar{3}n$, cubic $Fd\bar{3}m$, cubic $Ia\bar{3}d$, modulated structure, and a chiral mesostructure with helical arrangement of the pores, were successfully prepared based on this synthesis route,[4,9,17–19] though some of them have not been observed even in liquid-crystal systems.

Herein, we report a new mesoporous structure, AMS-10 (anionic surfactant templated mesoporous silica 10), which exhibits bicontinuous double diamond cubic $Pn\bar{3}m$ symmetry, prepared with anionic surfactant *N*-myristoyl-L-glutamic acid (C_{14}GluA) as template and *N*-trimethoxylsilylpropyl-*N*,*N*,*N*-trimethylammonium chloride (TMAPS) as CSDA. The packing of the micelle was controlled by simply adjusting the neutralization degree of the C_{14}GluA surfactant.

Different mesophases ranging from tetragonal $P4_2/mnm$ (cage type, AMS-9), cubic $Fd\bar{3}m$ (cage type, AMS-8), to 2D hexagonal *p6mm* (cylindrical, AMS-3), and an unknown mesophase (denoted as AMS-10) were obtained by decreasing the amount of NaOH that was added into the reaction system (Figure 1). The neutralization degree of the surfactant increased with the amount of NaOH that was added into the system. The first three types of mesostructure were characterized by high-resolution transmission electron microscopy (HRTEM; see Supporting Information). They gave many reflections with similar magnitude of scattering vectors, and these reflections could only be resolved by a single-crystal experiment. Their electron diffractions were separately observed as a single-crystal experiment and are consistent with their XRD patterns. It is inferred that AMS-10 may exhibit a lower curvature close to bicontinuous cubic $Ia\bar{3}d$ from the sequence of the mesophases.

The XRD pattern of AMS-10 shows two intense and well-resolved peaks in the range $1° < 2\theta < 2°$ with a *d* spacing ratio of about $\sqrt{3}/\sqrt{2}$, which is quite rare in the mesoporous silica reported earlier. We can index the two peaks by any crystal systems. If it is assumed as cubic, the two peaks can be indexed to 110 and 111 reflections, or to 200 and 211 reflections, and so on. From a set of electron diffraction patterns or HRTEM images, we can conclude that the crystal belongs to the cubic system. The HRTEM images taken with the [100], [110], and [111] incidences are shown in Figure 2. The Fourier transform diffractogram of the image of [100] incidence shows the reflection conditions $0kl$: $k + l = 2n$ and $00l$: $l = 2n$, and that of the [110] incidence shows the conditions *hkl*: none and *hhl*: none. From these results, two space groups are possible, $Pn\bar{3}$ (201) or $Pn\bar{3}m$ (224). The space group $Pn\bar{3}m$ was chosen because of its high symmetry. Thus, the first two peaks of the XRD pattern can be concluded to be 110 and 111 reflections based on a cubic

[*] Dr. Y. Sakamoto, Prof. O. Terasaki
Structural Chemistry
Arrhenius Laboratory
Stockholm University
10691 Stockholm (Sweden)
Fax: (+46) 816-3118
E-mail: yasuhiro@struc.su.se
C. Gao, Prof. S. Che
School of Chemistry and Chemical Technology
State Key Laboratory of Composite Materials
Shanghai Jiao Tong University
800 Dongchuan Road, Shanghai 200240 (P.R. China)
Fax: (+86) 21-5474-1297
E-mail: chesa@sjtu.edu.cn
Dr. K. Sakamoto
Research Center, Shiseido Co., LTD
2-2-1, Hayabuchi, Tsuzuki-ku, Yokohama 224-8558 (Japan)

[**] This work was supported by the National Natural Science Foundation of China (grant no. 20425102 and 20521140450), the China Ministry of Education, and the Shanghai Science Foundation (0452nm061 and 05XD14010). O.T. thanks the Swedish Science Research Council (VR) and Japan Science and Technology Agency (JST) for financial support.

Supporting information for this article is available on the WWW under http://www.angewandte.org or from the author.

 © 2006 Wiley-VCH Verlag GmbH & Co. KGaA, Weinheim

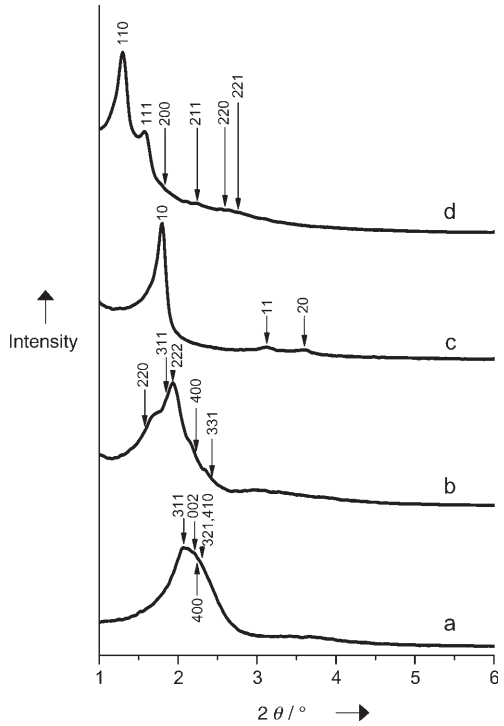

Figure 1. XRD patterns of calcined mesoporous silica prepared with C_{14}GluA as surfactant and TMAPS as CSDA and by precisely adjusting the acidity of the reaction system. The compositions of the gels are C_{14}GluA/TMAPS/TEOS/H_2O/NaOH = 1:1.5:15:1983:*x*; a) *x* = 2 ($P4_2/mnm$), b) *x* = 1.5 ($Fd\bar{3}m$), c) *x* = 1 ($p6mm$), and d) *x* = 0.75 ($Pn\bar{3}m$; AMS-10).

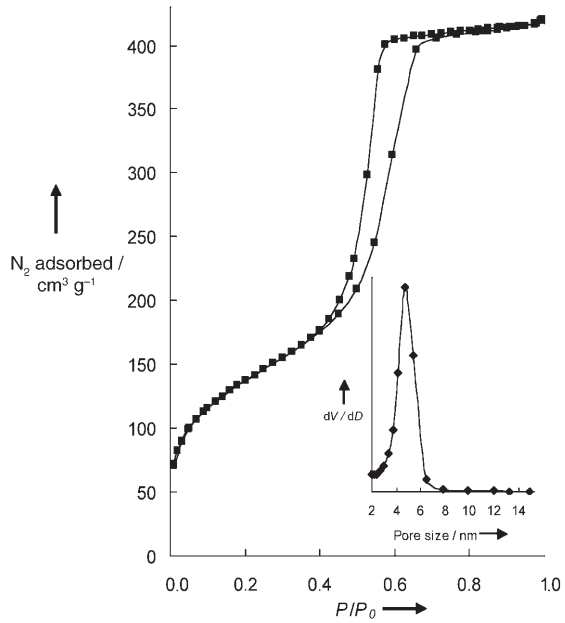

Figure 3. Nitrogen adsorption isotherm and pore size distribution (calculated by the BJH method based on the adsorption branch) of the calcined mesoporous silica AMS-10.

$Pn\bar{3}m$ space group, and it can be calculated from the 110 peak that the unit cell of AMS-10 is 9.6 nm. Also, the mesophase is highly ordered as can be derived from the large uniform areas of the HRTEM images.

Nitrogen adsorption and desorption isotherms of AMS-10 (Figure 3) show a typical type IV isotherm with an evident hysteresis loop in the range $0.45 < P/P_0 < 0.7$. The specific surface area and pore volume of the material are 493 $m^2 g^{-1}$ and 0.65 $cm^3 g^{-1}$, respectively. The pore diameter is about 4.7 nm calculated by the BJH method based on the adsorption branch of the isotherm, which is larger than that of common mesophases prepared with anionic surfactants.

A 3D reconstruction of the structure was conducted on the basis of the analysis of Fourier diffractograms taken from TEM images along high-symmetry zone axes of AMS-10. Table 1 shows crystal structure factors, both amplitude and phase, extracted from thin parts of crystals along three different zone axes, namely the [100], [110], and [111] directions. The origin of the symmetry was taken at the inversion center of $Pn\bar{3}m$ (origin choice 2); that is, the phase should be 0 or π. The electrostatic potential density map of AMS-10 was obtained by taking inverse Fourier summation of these crystal structure factors (not shown here). With a silica density of about 2.2 $g cm^{-3}$ and a pore volume of 0.65 $cm^3 g^{-1}$ from nitrogen adsorption data, the 3D pore structure of AMS-10 was determined (Figure 4a). The pore volume fraction therein corresponds to 58.8%. It can be calculated that AMS-10 has a pore diameter of 4.6 nm and wall thickness of 2.2 nm, values that are consistent with those calculated from nitrogen adsorption measurements. As can be

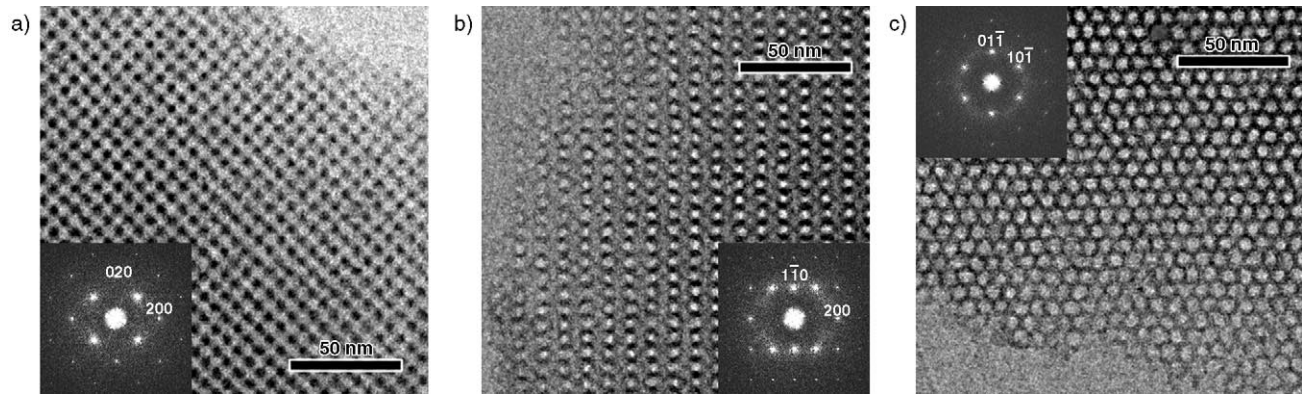

Figure 2. HRTEM images and Fourier diffractograms of the calcined mesoporous silica AMS-10. The images were taken along the zone axes as follows: a) [100], b) [110], and c) [111].

© 2006 Wiley-VCH Verlag GmbH & Co. KGaA, Weinheim

Table 1: Crystal structure factors (amplitudes and phases) extracted from HRTEM images of calcined AMS-10 ($a = 9.6$ nm).

h	k	l	$h^2+k^2+l^2$	d [nm]	Amplitude	Phase
1	1	0	2	6.80	100.00	π
1	1	1	3	5.55	57.09	0
2	0	0	4	4.81	13.13	0
2	1	1	6	3.92	3.40	π
2	2	0	8	3.40	0.79	π
2	2	1	9	3.20	0.57	0
3	1	0	10	3.04	0.42	π
3	1	1	11	2.90	0.06	0
2	2	2	12	2.77	0.20	π
3	2	1	14	2.57	0.13	0
4	0	0	16	2.40	0.10	0
3	2	2	17	2.33	0.10	π
3	3	0	18	2.27	0.07	0
4	2	0	20	2.15	0.01	π
4	3	3	34	1.65	0.05	0
4	4	2	36	1.60	0.02	0
7	1	0	50	1.36	0.01	0
6	3	3	51	1.35	0.01	0

seen from Figure 4a, b, the silica wall of the AMS-10 follows a typical diamond minimal surface (D surface) in analogy to the gyroid minimal surface (G surface) as observed for the silica wall of MCM-48.[12] From this result, we conclude that AMS-10 has a bicontinuous structure composed of an enantiomeric pair of 3D mesoporous networks that are interwoven as shown in Figure 4c. Each network, which is divided by a D surface, consists of tetrahedral connection of pores at the $\bar{4}3m$ position, 2*a* site (Wyckoff notation), although in the case of a bicontinuous cubic $Ia\bar{3}d$ structure each network that is divided by a G-surface consists of three connected pores at the 32 position, 16*b* site (Wyckoff notation).

The surfactants C_nGluA ($n = 12$–18) with different chain lengths also gave rise to the ordered bicontinuous cubic $Pn\bar{3}m$ mesostructure in combination with either TMAPS or 3-aminopropyltrimethoxylsilane (APS). The neutralization degree of the surfactant is crucial to form the specific mesophase in both synthesis systems. The effect of the neutralization degree on the formation of mesostructures can be explained in terms of the surface charge density (σ) of the surfactant micelles, which increases with the amount of NaOH added into the carboxylic acid surfactant solution. It is useful to introduce the surfactant packing parameter, $g = v/a\,l$, where v is the chain volume, a is the effective hydrophobic/hydrophilic interfacial area, and l is the chain length.[20] The lower charge density contributes to a partial decrease in the electrostatic repulsion between the charged surfactant head groups and a decrease in the effective head group area of surfactant, a, therefore resulting in an increase in the g value. It is well-known that the g parameter of lyotropic liquid-crystal phases increases in the order: micellar tetragonal $P4_2/mnm$, micellar cubic $Fd\bar{3}m <$ cylindrical 2D hexagonal $p6mm <$ bicontinuous cubic $Pn\bar{3}m$.[21] Thus, it is reasonable that a lower charge density of the micelle surface facilitates the formation of the cubic $Pn\bar{3}m$ mesophase with a larger g parameter.

In summary, mesoporous silica AMS-10 with a novel bicontinuous cubic mesophase $Pn\bar{3}m$ was synthesized by using an anionic surfactant as template. Detailed characterizations were performed through XRD, HRTEM, and nitrogen adsorption studies, and a 3D structure was derived from these results and those obtained through electron crystallography. Precise control of the neutralization degree of the anionic surfactant is key to the synthesis of AMS-10 and also proves a feasible and simple means to achieve mesophase control of anionic surfactant templated mesoporous silica (AMS). Because of its characteristic mesoporous structure, this bicontinuous cubic mesoporous material could be useful, for example, as biocompatible materials for the encapsulation, controlled release, and delivery of drugs and biomolecules.

Experimental Section

TMAPS (Azmax) and tetraethyl orthosilicate (TEOS; TCI) were purchased and used as received. The synthetic method of glutamic acid derived surfactant C_{14}GluA is described in the Supporting Information.

In a typical synthesis of AMS-10, NaOH (7.5 g of 0.1 mol L^{-1} solution) was added to a solution of C_{14}GluA (0.357 g, 1 mmol) in deionized water (28.2 g) stirring at 60 °C. After the solution became homogeneous a mixture of TMAPS (0.773 g; 50% in methanol,

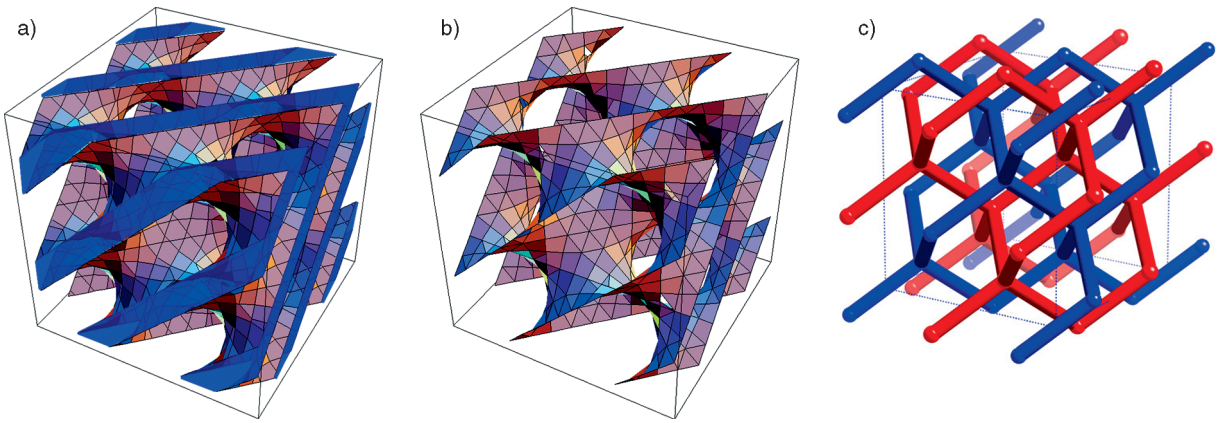

Figure 4. 3D structure of a) the bicontinuous cubic $Pn\bar{3}m$ mesoporous silica AMS-10 (as derived from electron crystallography), b) the D surface, and c) the 3D networks of double diamond structure divided by the D surface. They show a 2×2×2 unit cell.

 © 2006 Wiley-VCH Verlag GmbH & Co. KGaA, Weinheim

1.5 mmol) and TEOS (3.12 g, 15 mmol) was added, and the mixture was stirred at 60 °C for 10 min. The molar composition of the final gel was C_{14}GluA/TMAPS/TEOS/H_2O/NaOH = 1:1.5:15:1983:0.75. The reaction system was then kept static for 2 days at 60 °C to allow the product to hydrolyze, condense, and age. To remove the surfactant, the as-synthesized mesoporous silica was calcined at 550 °C for 6 h or extracted using a mixture of HCl (37 wt %) and ethanol (90 % w/w) for 12 h.

XRD patterns were recorded on a Rigaku X-ray diffractometer D/MAX-2200/PC with $Cu_{K\alpha}$ radiation (40 kV, 20 mA) at a rate of 1.0 deg min^{-1} over the range of $1° < 2\theta < 6°$. HRTEM was performed with a JEOL JEM-3010 microscope operating at 300 kV (Cs = 0.6 mm, point resolution 1.7 Å). Images were recorded with a CCD camera (MultiScan model 794, Gatan, 1024 × 1024 pixels, pixel size 24 × 24 μm^2) at 50000–80000 magnification under low-dose conditions. The adsorption/desorption isotherms were measured with an ASAP2100 using N_2 as adsorbate at 77 K. The specific surface area was calculated by the BET method, and the pore size was obtained from the maxima of the pore size distribution curve calculated by the BJH method by using the adsorption branch of the isotherm.

Received: November 18, 2005
Revised: February 11, 2006
Published online: May 26, 2006

Keywords: electron diffraction · electron microscopy · mesoporous materials · surfactants · template synthesis

[1] T. Yanagisawa, T. Shimizu, K. Kuroda, C. Kato, *Bull. Chem. Soc. Jpn.* **1990**, *63*, 988–992.
[2] J. S. Beck, J. C. Vartuli, W. J. Roth, M. E. Leonowicz, C. T. Kresge, K. D. Schmitt, C. T.-W. Chu, D. H. Olson, E. W. Sheppard, S. B. McCullen, J. B. Higgins, J. L. Schlenkert, *J. Am. Chem. Soc.* **1992**, *114*, 10834–10843.
[3] S. Shen, A. E. Garcia-Bennett, Z. Liu, Q. Lu, Y. Shi, Y. Yan, C. Yu, W. Liu, Y. Cai, O. Terasaki, D. Zhao, *J. Am. Chem. Soc.* **2005**, *127*, 6780–6787.
[4] A. E. Garcia-Bennett, N. Kupferschmidt, Y. Sakamoto, S. Che, O. Terasaki, *Angew. Chem.* **2005**, *117*, 5451–5456; *Angew. Chem. Int. Ed.* **2005**, *44*, 5317–5322.
[5] Q. Huo, R. Leon, P. M. Petroff, G. D. Stucky, *Science* **1995**, *268*, 1324–1327.
[6] Q. Huo, D. I. Margolese, U. Ciesla, P. Feng, T. E. Gier, P. Sieger, R. Leon, G. D. Stucky, *Nature* **1994**, *368*, 317–321.
[7] Y. Sakamoto, M. Kaneda, O. Terasaki, D. Zhao, J. M. Kim, G. D. Stucky, H. J. Shin, R. Ryoo, *Nature* **2000**, *408*, 449–453.
[8] S. Shen, Y. Li, Z. Zhang, J. Fan, B. Tu, W. Zhou, D. Zhao, *Chem. Commun.* **2002**, 2212–2213.
[9] A. E. Garcia-Bennett, K. Miyasaka, O. Terasaki, S. Che, *Chem. Mater.* **2004**, *16*, 3597–3605.
[10] D. Zhao, Q. Huo, J. Feng, B. F. Chmelka, G. D. Stucky, *J. Am. Chem. Soc.* **1998**, *120*, 6024–6036.
[11] a) Y. Sakamoto, I. Díaz, O. Terasaki, D. Zhao, J. Pérez-Pariente, J. M. Kim, G. D. Stucky, *J. Phys. Chem. B* **2002**, *106*, 3118–3123; b) J. Fan, C. Yu, F. Gao, J. Lei, B. Tian, L. Wang, Q. Luo, B. Tu, W. Zhou, D. Zhao, *Angew. Chem.* **2003**, *115*, 3254–3258; *Angew. Chem. Int. Ed.* **2003**, *42*, 3146–3150.
[12] A. Carlsson, M. Kaneda, Y. Sakamoto, O. Terasaki, R. Ryoo, S. H. Joo, *J. Electron Microsc.* **1999**, *48*, 795–798.
[13] a) A. C. Finnefrock, R. Ulrich, A. Du Chesne, C. C. Honeker, K. Schumacher, K. K. Unger, S. M. Gruner, U. Wiesner, *Angew. Chem.* **2001**, *113*, 1247–1251; *Angew. Chem. Int. Ed.* **2001**, *40*, 1207–1211; b) A. Jain, G. E. S. Toombes, L. M. Hall, S. Mahajan, C. B. W. Garcia, W. Probst, S. M. Gruner, U. Wiesner, *Angew. Chem.* **2005**, *117*, 1252–1255; *Angew. Chem. Int. Ed.* **2005**, *44*, 1226–1229.
[14] a) I. Honma, H. S. Zhou, D. Kundu, A. Endo, *Adv. Mater.* **2000**, *12*, 1529–1533; b) S. A. El-Safty, T. Hanaoka, *Chem. Mater.* **2003**, *15*, 2892–2902.
[15] D. Zhao, Q. Huo, J. Feng, J. Kim, Y. Han, G. D. Stucky, *Chem. Mater.* **1999**, *11*, 2668–2672.
[16] D. Zhao, J. Feng, Q. Huo, N. Melosh, G. H. Fredrickson, B. F. Chmelka, G. D. Stucky, *Science* **1998**, *279*, 548–552.
[17] S. Che, A. E. Garcia-Bennett, T. Yokoi, K. Sakamoto, H. Kunieda, O. Terasaki, T. Tatsumi, *Nat. Mater.* **2003**, *2*, 801–805.
[18] A. E. Garcia-Bennett, O. Terasaki, S. Che, T. Tatsumi, *Chem. Mater.* **2004**, *16*, 813–821.
[19] S. Che, Z. Liu, T. Ohsuna, K. Sakamoto, O. Terasaki, T. Tatsumi, *Nature* **2004**, *429*, 281–284.
[20] J. N. Israelachvili, D. J. Mitchell, B. W. Ninham, *J. Chem. Soc. Faraday Trans. 2* **1976**, *72*, 1525–1568.
[21] J. M. Seddon, J. Gulik-Krzywicki, H. Delacroix, *Phys. Chem. Chem. Phys.* **2000**, *2*, 4485–4493.

 © 2006 Wiley-VCH Verlag GmbH & Co. KGaA, Weinheim